Research Article
doi.org/10.1002/cplu.202100507

Chemistry Europe
European Chemical Societies Publishing

www.chempluschem.org

Poly(arylisocyanides) as Versatile, Enantiodiscriminating Alignment Media for Small Molecules

Svenja Wesp, Kai Wolf, Stefan Immel, and Michael Reggelin*[a]

In memory of Klaus Hafner.

Lyotropic liquid crystalline (LLC) phases of amino acid derived polyarylisocyanides were employed as chiral alignment media for the measurement of residual dipolar couplings (RDCs) of small chiral organic molecules. Anisotropic samples in $CDCl_3$ displayed quadrupolar splittings of the deuterium signal in the range of several hundreds of Hertz. The LLC phases showed excellent orienting properties for a broad range of analytes bearing various functional groups. The precise extraction of RDCs in the range of up to ± 40 Hertz from F2-coupled HSQC spectra was possible. Additionally, the chiral environment offers the opportunity for diastereomorphous interactions with the enantiomers of chiral analytes leading to two different sets of RDCs. This differential order effect was particularly pronounced with ketones and alcohols.

Introduction

Amongst other anisotropic NMR parameters residual dipolar couplings (RDCs) have widely been used in structure elucidation, not only of biological macromolecules but also of small molecules.[1] They are a powerful tool for solving conformational and configurational problems in structural analysis[1f,h,j,k,q,2] in which they are mostly considered as a source of additional information including cases were they played the dominant role and conventional NMR parameters like NOE or scalar couplings failed to solve the problem.[3] Contrary to the latter, RDCs deliver structural information without the necessity of an empiric parametrization, as is the case for the evaluation of scalar couplings.[4] Furthermore, as global parameters, RDCs do not rely on short-ranged interactions like cross relaxation (nuclear Overhauser effect, NOE)[5] or cross-correlated relaxation.[6]

However, as RDCs are anisotropic NMR parameters, it is necessary to orient the analyte molecules in the magnetic field for their observation. This is usually done by so-called alignment media, aiming for RDCs in the order of 10^{-3} of the maximum dipolar coupling (*weak alignment*). Unlike in solid state NMR under these conditions RDCs are easily accessible as a contribution to the C–H *J*-coupling (e.g. ${}^1T_{CH} = {}^1J_{CH} + 2 \cdot {}^1D_{CH}$). In the standard procedure, the extracted RDCs are evaluated by an appropriate software to calculate the so-called alignment tensor.[7] With this tensor and a structural model in hand, it is possible to back-calculate dipolar couplings and verify – or falsify – a given structural proposal. Recently, a conceptionally different approach (implemented into the new software ConArch$^+$)[8] has been introduced avoiding this verification or falsification of calculated structures. Herein, starting structures of an arbitrary configuration evolve under the influence of all types of isotropic and anisotropic NMR-data into final structures of correct relative configuration.[1b,8–9]

There are mainly two approaches to generate weak alignment, namely the use of stretched or compressed polymer gels (SAG = strain induced alignment in a gel)[1e,10] and lyotropic liquid-crystalline (LLC) phases.[11] Both systems allow for the determination of RDCs, albeit in a different manner.

In the field of anisotropic NMR on biological macromolecules the configuration of the stereogenic centers is mostly well known, e.g. for peptides or proteins, which typically consist of L-configured amino acids. This is not the case for small molecules, as they are the products of frequently unknown synthetic pathways including stereogenic steps and building blocks of unknown configurations. For such problems, not only a differentiation of diastereomers is necessary, but also the assignment of enantiomers in case of chiral analytes may appear as a particularly difficult task. This entails the necessity that one has to provide an anisotropic environment in such a way, that diastereomorphic interactions between analyte and alignment media can occur. This is obviously the case only if the orienting medium is chiral and non-racemic itself. As a consequence a differential order effect (DOE)[12] may occur resulting in two discrete sets of dipolar couplings leading to two different alignment tensors, one for each enantiomer.

Of course, this is a necessary but not a sufficient precondition to determine the absolute configuration of a chiral compound. As with all other NMR-methods used to distinguish between enantiomers like chiral solvating agents (CSA) or chiral shift reagents (CSR) the observed effect does not directly permit an absolute configurational assignment. This may be possible if one would be able to calculate the alignment tensor for each enantiomer and compare the result with the experiment. To

[a] *Dr. S. Wesp, Dr. K. Wolf, Dr. S. Immel, Prof. Dr. M. Reggelin*
Technische Universität Darmstadt
Clemens Schöpf Institut für Organische Chemie und Biochemie
Alarich-Weiss-Str. 4, 64287 Darmstadt (Germany)
E-mail: re@chemie.tu-darmstadt.de

Supporting information for this article is available on the WWW under https://doi.org/10.1002/cplu.202100507

facilitate this problem, it is obvious to make efforts maximizing the DOE in such a way that even crude theoretical models may be sufficient to provide a decision based on this tensor comparison.

An increasing number of enantiodifferentiating LLC-based alignment media for organic solvents have been developed in recent years. Besides the well-established homopolypeptides poly-γ-benzyl-L/D-glutamate (PBLG/PBDG), poly-γ-ethyl-L-glutamate (PELG/PEDG), and poly-ε-carboxybenzoyl-L/D-lysin (PCBLL/PCBDL)[2f,11l,n,12–13] only a few chiral non-peptidic polymers are known, amongst them LLC phases based on polyguanidines[14] and polyacetylenes.[11b,h,15] Moreover, SAG media like polyacrylamides,[10f] e-gelatin.[16] and cross-linked PBLG[10e] have been introduced as chiral orienting media.

In 2012 Berger and co-workers introduced an *L-alanine* derived polyarylisocyanide[17] as a new alignment medium for organic solvents.[18] Although the authors mentioned a prospective enantiodifferentiating capability, this aspect was not investigated. The same is true for the polyisocyanopeptides[19] studied by Lei and Sun in 2017.[20]

Encouraged by our results with amino acid side chain bearing polyarylacetylenes,[11b,15b] we decided to investigate the potential of structurally closely related helically chiral polyarylisocyanides[21] as enantiodifferentiating alignment media. To learn as much as possible about the orienting properties of the corresponding LLC-phases, we examined 11 different analytes, including carboxylic acids, ketones, aldehydes, alcohols, amines and unsaturated hydrocarbons. Moreover, also the influence of the amino acid side chain was investigated by choosing *L-alanine* and *L-valine* as the amino acids in the repeating units of the polymers.

Results and Discussion

Monomer synthesis and polymer characterization

The synthesis of both enantiomers of the monomers **1** and **2** was achieved in five steps by modified procedures based on work published earlier[21c,22] with an overall yield of 43% for **1**/*ent*-**1** and 40% for **2**/*ent*-**2** respectively (Scheme 1).

Polymerization was achieved in THF/ethanol mixtures by the Ni-initiated merry-go-round mechanism[23] reactions according to the work of Yashima,[21c] resulting in yellow polymers **p1** and **p2**. Even though the polymers derived from the enantiomeric monomers *ent*-**1** and *ent*-**2** respectively, may slightly differ in molecular weight and polydispersity, they can be treated as enantiomers of **p1** and **p2** to a good approximation. In total, two different preparations for **p1** and **p2** as well as one each for the enantiomers (**p1a-b**, **p2a-b**, *ent*-**p1**, *ent*-**p2**) were synthesized in order to prove the reproducibility of the NMR-experiments described in the following (a detailed description of the syntheses and the polymer characterizations can be found in the SI).

Due to their high helix inversion barriers, polyisocyanides belong to the so-called static helical polymers.[21a] Very much like the polyguanidines studied by Novak[24] and ourselves,[14]

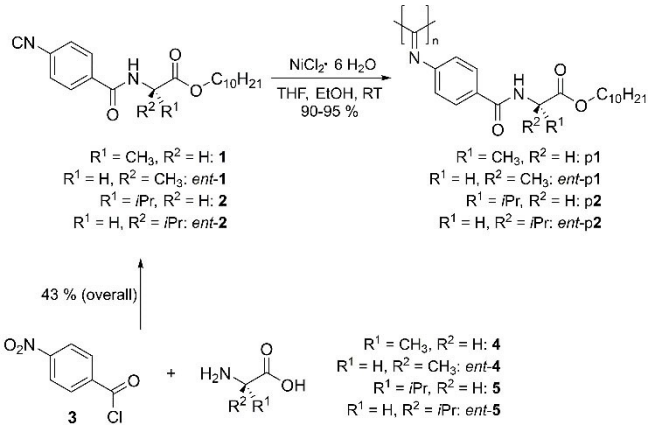

Scheme 1. Synthesis and polymerization of the isocyanide monomers **1** and **2** and their enantiomers.

the pristine polymer generated immediately after the polymerization reaction is in a so-called kinetically controlled conformation (KCC). In most cases, this conformation is not the one with maximum helicity in the polymer backbone. To reach this state a thermal treatment (annealing) may transform the system into a thermodynamically controlled conformation (TCC) which frequently is the one with a higher stereoregularity.

For this reason and to guarantee that every NMR-measurement is based on a polymer in a comparable structural state, we annealed the polymers for several days (see SI 3.1 for details) in toluene at 100 °C (Figure 1). The success and the endpoint of this thermal treatment was judged by monitoring the time dependence of the CD-signal at around 360 nm. In accordance with Yashimas earlier observations, the *L-alanine* derived polymer **p1** was generated with a slight left-helical excess, which developed during the annealing procedure into a TCC with a predominantly left-handed backbone (Figure 1a).[21c] As expected, the opposite behavior was observed with the enantiomeric polymer *ent*-**p1**.

To our surprise, the L-*valine*-derived polymer **p2** behaves completely different (Figure 1b). Although the KCC of this polymer is also weakly left-handed, it develops under helix reversal into a pronounced right-handed helix with a Θ_{max} at 360 nm being close to the one of **p1** but with inverted sign. This means that the same absolute configuration at the α-carbons of the amino acids induce the opposite helical configuration of the annealed polymer backbone.

Orienting properties of the polymers

All polymers form lyotropic liquid crystalline phases in $CDCl_3$ with a critical concentration at room temperature of approximately 13% (w/w) for **p1**/*ent*-**p1** and 7% (w/w) for **p2**/*ent*-**p2**, respectively. The phase transitions were monitored by measur-

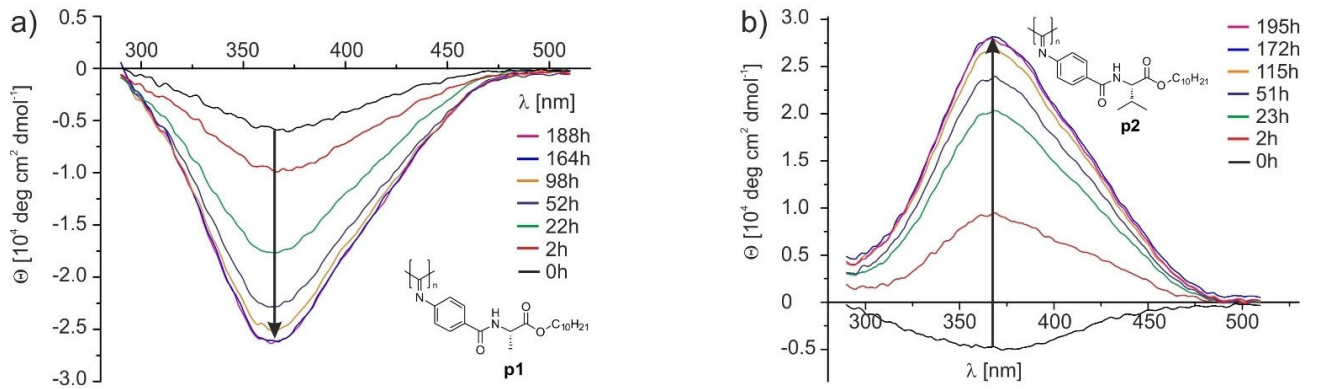

Figure 1. Time dependence of the intensity of the first cotton-effect during the thermal annealing of the polymers **p1-a** and **p2-a** in toluene at 100 °C. a) For the *alanine* derived polymer **p1**, the originally induced helical sense (left handed) remains the same but the helicity increases strongly. b) The *valine* derived polymer **p2** on the contrary changes its helical sense from weakly left-handed to strongly right-handed.

ing ^{2}H-NMR spectra of the LLC phases including a DMSO-d_6 capillary as an external standard. The deuterium signal of the deuterated chloroform showed either a singlet (isotropic solution) or a doublet caused by the quadrupolar coupling ($\Delta\nu_Q$) in the anisotropic LLC-phase. Close to the critical concentration, **p1**/*ent*-**p1** forms a biphasic system consisting of an isotropic and an anisotropic phase. Thus, the simultaneous measurement of isotropic and anisotropic parameters with a single sample is possible, as previously described.[11e]

The phases formed in a 16% solution of **p1** and a 10% solution of **p2** in $CDCl_3$ were stable between 250 K and 320 K with a strong temperature dependence of the quadrupolar splitting (Figure 2). Moreover, at the given concentrations, the *alanine* derived phase (**p1**) gives rise to considerably higher values for the splitting than the *valine* derived one (**p2**), which leads to the expectation that the degree of orientation in the former is higher than in the latter.

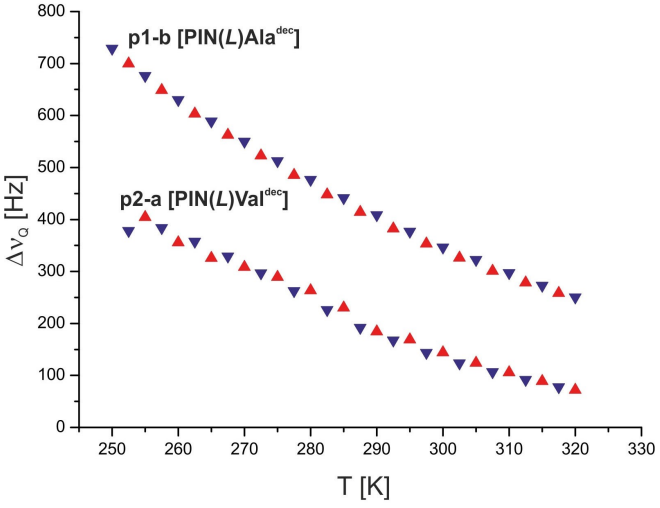

Figure 2. Temperature dependence of the quadrupolar splitting $\Delta\nu_Q$ of LLC phases of **p1-b** (16% w/w) and **p2-a** (10% w/w). Red triangles denote data points measured during heating, blue triangles during cooling.

We started our study on the orienting properties of these phases with both enantiomers of isopinocampheol (IPC). This terpene alcohol was chosen for a number of reasons. It is a conformational rigid bicyclic system displaying well-separated signals in its ^{1}H- as well as the ^{13}C-spectrum. Moreover, it is commercially available in both enantiomeric forms and has been used by many other groups to judge the orienting properties of new alignment media.

Therefore, t_2-coupled HSQC spectra of both IPC enantiomers in LLC phases of **p1** and **p2** were measured, using the CLIP-HSQC pulse sequence introduced by Luy.[25]

The resulting spectra showed pleasantly narrow lines, which allows a precise extraction of RDCs by the determination of the total coupling constants ($^{1}T_{CH}$) together with the known scalar couplings ($^{1}J_{CH}$) without the occurrence of any strong coupling artifacts (Figure 3). Gratifyingly, both polymers were able to align IPC in a satisfactory manner, resulting in RDCs within a range of $|^{1}D_{CH}| \leq 39$ Hz for **p1-b** (~16%w/w; $\Delta\nu_Q \sim 500$ Hz) and $|^{1}D_{CH}| \leq 10$ Hz for **p2-b** (~14%w/w; $\Delta\nu_Q \sim 300$ Hz) respectively (see SI 5).

The experimental RDCs ($^{1}D_{exp}$) together with DFT optimized structures (B3LYP/6-311+G(d,p)) were used to calculate the alignment tensor by singular value decomposition[26] using our recently developed software package *ConArch*$^{+}$.[1a,b,8–9] Following the standard procedure for the verification or falsification of structure models, the alignment tensor serves as a basis to back-calculate theoretical RDCs.[7] The quality of fit of experimental and back-calculated RDCs forms the basis for the decision in favor or against the model. Usually this is done by comparing Pearson correlation coefficients, scaled versions thereof like the Cornilescu *Q*-factor[27] or the Akaike information criterion (AIC-values).[28] Although common practice, this procedure may fail because both the experimental and *especially* the back-calculated couplings are afflicted with errors.[9] The latter couplings are affected by the quality of the structure models used for their calculation, which is particularly important when

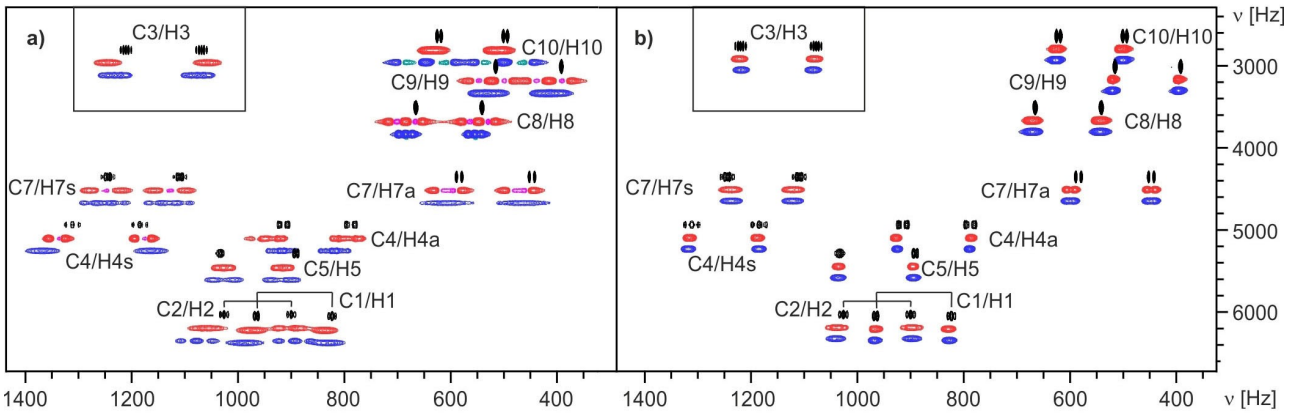

Figure 3. a) 125 MHz CLIP-HSQC spectra of (+)-IPC in isotropic solution (500 MHz, 300 K, $CDCl_3$, black contours), (+)-IPC in 16% (w/w) **p1-b** (red) and (−)-IPC in 16% (w/w) **p1-b** (blue). b) 125 MHz CLIP-HSQC spectra of the enantiomers of IPC in 14% (w/w) **p2-b** (same color encoding as for the samples in **p1**. Only the cross peaks of the isotropic samples (black contours) have their correct spectral position with respect to $CDCl_3$. The other peaks have been shifted to avoid overlap.

diastereomers with their respective conformational spaces are compared.

This problem does not occur when the orientational differences of two enantiomers in a homochiral alignment medium are to be compared. In this case, the reference structure is the same and, therefore a potential difference in the alignment tensors can be used as a measure for the capability of the chiral medium to differentiate the enantiomers of a given chiral analyte. For this purpose the intertensor angle β or its cosine (generalized cosine beta: GCB) is calculated[7] in which a GCB of $\cos\beta = 1$ means no differentiability, whereas a GCB of $\cos\beta = 0$ means maximum difference of the tensor orientations.

For (+)- and (−)-IPC two different sets of RDCs and consequently two different alignment tensors were obtained from the HSQC measurements in **p1-b**. The GCB for these two tensors was found to be 0.45 indicating a pronounced enantiodifferentiating capability (or DOE) of the medium (Table 1, #1/2).[29] The same is true for the *valine* derived polymer **p2-b**, although the effect was much smaller (GCB = 0.90).

To learn more about the capability of the polyisonitrile based LLC-phases not only to differentiate between enantiomers but also about their functional group tolerance, we investigated the orientational behavior of 11 different analytes displaying various functional groups including alcohols (menthol, fructoseacetonide), aldehydes (perilla aldehyde), ketones (carvone, camphor), amines (nicotine, strychnine, sparteine) and hydrocarbons (α-pinene, β-caryophyllene; Table 1).

Exact sample compositions, coupling constants and fit parameters for all analyte/alignment medium combinations can be found in the SI (Table S2). For analytes available in both enantiomeric forms, media with identical stereogenic elements were used to determine the respective GCB-values. For compounds available only in one enantiomeric form, we generated the diastereomorphous interaction by orienting them in LLC phases of inverted stereogenic elements (*ent*-**p1** and *ent*-**p2**).

The data in Table 1 discloses some trends concerning the orienting properties of the two media and their respective enantiomeric forms.

1) All analytes with the above-mentioned spectrum of functional groups are compatible with both LLC-phases.
2) Judged from the quadrupolar splitting of the deuterium signal of the chloroform solvent, which is much higher in *alanine*-derived **p1** than in *valine*-derived **p2** (and is significant even when taking the small differences in the polymer concentrations into account), one may get the impression that **p1** generally orients more strongly than **p2**. This is not the case as can be derived from the corresponding GDO values. For example, the small, spherical secondary alcohol IPC (#1/2) gets strongly oriented in **p1** (GDO ((+)-IPC = $12.6\cdot10^{-4}$)/(−)-IPC = $18.6\cdot10^{-4}$)) but much less in **p2** (GDO ((+)-IPC = $4.5\cdot10^{-4}$)/(−)-IPC = $5.0\cdot10^{-4}$)). On the other hand, the opposite is true for the fructose acetonide (#5/6), which is a 6-membered ring secondary alcohol too. This may be due to the elongated shape of the latter, entailing the conclusion that for the Val-polymer **p2** shape recognition may be more important than for the Ala-polymer (**p1**). In accordance with this expectation, sparteine (#21/22) with a large aspect ratio, against the common trend, gets stronger oriented in **p2** than in **p1**.The much stronger orientation of camphor (#11/12) in **p2** as compared to **p1** remains unclear at the time being.
3) In most cases, **p1** and **p2** orient analytes of the same absolute configuration quite differently (homochiral comparison, last column in Table 1). This is especially pronounced with alcohols, ketones and hydrocarbons. One may speculate that this can be traced back to the fact that the helical sense of **p1** is opposite to **p2** despite the same absolute configuration in the amino acid side chain as already described. This combination of stereogenic elements leads

Research Article
doi.org/10.1002/cplu.202100507

Chemistry Europe
European Chemical Societies Publishing

Table 1. Results from the investigation of 11 different analytes in anisotropic phases in $CDCl_3$ of **p1**, **p2** and their respective enantiomers.

Analyte	#	Formula[a]	*Alanine* based polymers **p1** and *ent*-**p1** Polymer[b]	wt.%	$\Delta\nu_Q$[c]	*GDO*[d]	|RDC|$_{min}$	|RDC|$_{max}$	**GCB**[e]	*Valine* based polymers **p2** and *ent*-**p2** Polymer[b]	wt.%	$\Delta\nu_Q$[c]	*GDO*[d]	|RDC|$_{min}$	|RDC|$_{max}$	**GCB**[e]	Ala/Val GCB[f]
(+)-IPC	0	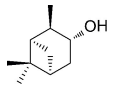	**p1-b**	15.94	555.8	12.6	1.45	23.80		***ent*-p2**	13.93	314.5	5.4	0.80	11.05		0.177
(+)-IPC	1		**p1-b**	15.94	555.8	12.6	1.45	23.80		**p2-b**	14.01	280.5	4.5	0.70	8.90		0.389
(−)-IPC	2		**p1-b**	15.96	572.4	18.6	4.65	39.05	**0.446**	**p2-b**	14.03	284.6	5.0	0.30	10.05	**0.902**	0.432
(+)-Menthol	3	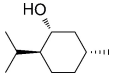	**p1-b**	16.04	543.5	9.2	4.20	14.30		**p2-b**	13.92	283.9	7.4	1.20	6.90		0.353
(−)-Menthol	4		**p1-b**	15.99	549.4	12.2	6.60	11.00	**0.435**	**p2-b**	14.01	277.9	7.2	1.00	15.80	**0.602**	0.411
	5		**p1-b**	15.89	643.3	10.9	1.20	5.00		**p2-b**	12.99	291.4	13.2	3.60	12.80		0.179
	6		*ent*-**p1**	16.04	539.0	8.6	1.60	16.80		*ent*-**p2**	13.99	336.1	10.2	4.00	20.30		0.501
Fructose acetonide		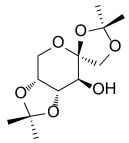							**0.522**							**0.768**	
(+)-α-Pinene	7		**p1-b**	15.94	567.5	3.9	0.30	6.05		**p2-b**	13.99	299.9	4.3	1.05	7.30		0.667
(−)-α-Pinene	8		**p1-b**	15.91	532.2	4.0	0.10	5.15	**0.979**	**p2-b**	13.97	284.9	4.1	0.15	7.40	**0.990**	0.744
	9		**p1-b**	15.99	596.7	13.2	2.00	15.30		**p2-b**	13.91	305.5	11.2	4.30	9.80		0.642
	10		*ent*-**p1**	16.06	510.6	7.8	0.90	13.50		*ent*-**p2**	14.00	306.1	11.8	4.40	10.20		0.782
β-Caryophyllene		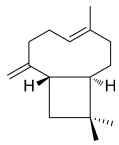							**0.677**							**0.993**	
(+)-Camphor	11		**p1-a**	16.02	466.7	5.1	0.55	9.55		**p2-a**	16.02	326.1	9.5	1.70	20.70		0.878
(−)-Camphor	12		**p1-a**	15.75	444.7	3.8	0.10	6.45	**0.897**	**p2-a**	16.06	321.0	9.4	0.70	20.10	**0.997**	0.776
(+)-Carvone	13	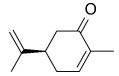	**p1-b**	16.02	628.3	9.6	0.80	6.10		**p2-b**	14.01	302.7	9.8	0.60	13.50		0.390
(−)-Carvone	14		**p1-b**	15.97	645.6	4.3	2.00	8.70	**0.481**	**p2-b**	13.98	297.7	10.2	1.30	13.60	**0.966**	0.044
	15	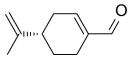	**p1-b**	15.98	642.3	14.2	3.05	12.42		**p2-b**	13.95	305.5	16.4	2.92	24.75		0.812
(−)-Perilla aldehyde	16		*ent*-**p1**	16.00	511.8	12.7	1.22	15.25	**0.928**	*ent*-**p2**	13.85	286.6	13.0	1.50	22.55	**0.639**	0.502
	17		**p1-b**	21.91	703.9	14.6	0.3	19.1		**p2-a**	14.02	233.4	17.6	0.15	41.70		0.920
	18		*ent*-**p1**	17.94	622.0	28.6	2.60	40.45		*ent*-**p2**	13.00	307.6	21.1	0.20	48.75		0.938
(−)-Strychnine		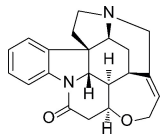							**0.807**							**0.990**	
	19	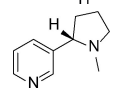	**p1-b**	16.00	620.6	19.6	2.90	28.80		**p2-b**	14.02	286.0	20.5	0.80	25.50		0.983
(−)-Nicotine	20		*ent*-**p1**	15.84	480.8	18.5	2.30	24.50	**0.986**	*ent*-**p2**	13.89	323.4	22.1	1.20	29.30	**0.998**	0.995
	21	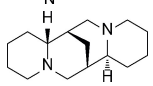	**p1-b**	15.98	605.2	9.3	1.15	9.60		**p2-b**	13.01	293.7	11.5	0.45	15.05		0.958
(−)-Sparteine	22		*ent*-**p1**	15.90	511.2	7.8	1.25	12.05	**0.953**	*ent*-**p2**	13.01	328.3	15.2	2.10	20.05	**0.991**	0.843

[a] The formulae display the (−)-enantiomer of the analytes, respectively. [b] For a detailed description of the polymers and the exact composition of the samples see SI (Table S2). [c] Quadrupolar splitting of the solvent. [d] GDO: *general degree of order* in units of [10^{-4}]. [e] Heterochiral comparison as a measure for enantiodifferentiation: either (+/−)-analyte/polymer or analyte/(+/−)-polymer. [f] Homochiral comparison as a measure for the difference in orientation induced by different polymers with the same configuration of the analyte.

to an interaction between the polymer and the analyte which would be diastereomorphic in nature when one neglects the constitutional difference of the amino acid side chains, thus emphasizing the stereochemical relations (e.g.: (+)-IPC | (S)-Ala | M-helix | | (+)-IPC | (S)-Val | P-helix). Interestingly, this seems not to be the case. The homochiral comparison of (+)-IPC aligned in left-handed **p1-b** and right-handed **p2-b** yielded a low GCB of 0.39. But, if one replaces **p2-b** by *ent*-**p2-b** which is also left-handed, then the GCB is even lower (0.18)! This in turn may be taken as an indication that the combination of different sidechain constitutions (Me *vs i*Pr) and configurations (*S*-Ala *vs R*-Val), together with the same helical sense of the polymer (M) generates a maximum difference in orientation.

4) The enantiodifferentiating capability of the *alanine* derived polymer **p1** is generally more pronounced than that of the *valine*-derived polymer **p2** (especially with the alcohols; see also Figure 4).
5) In both phases it is possible to orient olefinic hydrocarbons like α-pinene and β-caryophyllene, whereby the latter is surprisingly strong enantiodifferentiated in **p1** (GCB = 0.68!).
6) Noteworthy enantiodifferentiation with ketones occurs only with **p1**. Especially the enantiomers of carvone orient very different in **p1-b** (GCB = 0.48).
7) Given the fact that amino acid derived polyisocyanides stabilize their helical structure by H-bonding, it is remarkable that both phases are stable to a number of bases (strychnine, nicotine, sparteine). Even with perilla *acid* in **p1** we were able to evaluate HSQC spectra and extract RDCs. Unfortunately, we got only five which makes a calculation and comparison of the alignment tensors useless.
8) If one compares the polyisocyanides discussed here with the orienting properties of the polyacetylenes with identical side chains described earlier,[15b] it is very interesting to note that despite a roughly tenfold larger quadrupolar splitting of the former, the RDCs measured with the same analytes are of comparable magnitude. With **p1** and **p2** the RDCs are in the range of 1 to 10% of the quadrupolar splitting whereas with the polyacetylenes they are between 10 and 70% of $\Delta\nu_Q$. This means that there is no obvious correlation between the alignment strength felt by the solvent $CDCl_3$ and the analytes, which in turn means that cross-polymer comparisons of orientational properties based on the quadrupolar splitting of the solvent are invalid!

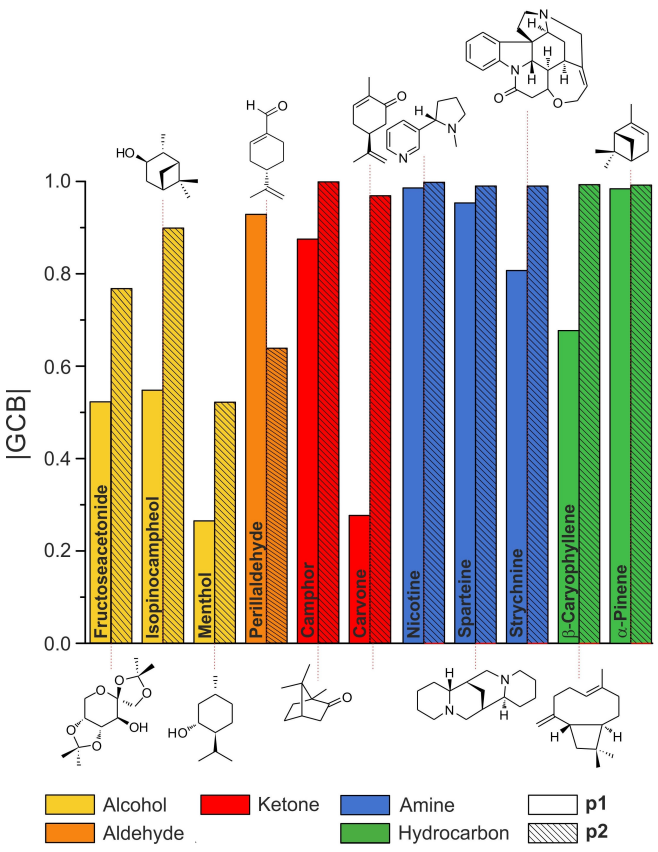

Figure 4. GCB plot for the investigated analytes in *alanine*- (filled) and *valine*-derived (shaded) polyisocyanides **p1** and **p2**, respectively.

Conclusion

The orienting properties and enantiodifferentiating capability of lyotropic liquid crystalline (LLC) phases formed in concentrated $CDCl_3$-solutions of two helically chiral polyarylisocyanides and their enantiomeric pendants were investigated. Despite the identical absolute configuration of the side chain stereogenic centers, after thermal annealing, the *L-alanine* derived polymer **p1** forms a left-handed helix whereas the polymer with L-*valine* derived side chains **p2** forms a right-handed helix. The functional group tolerance of the LLC-phases was studied using a set of 11 different analytes displaying a broad range of different functional groups. Both phases were compatible with all analytes including aliphatic and aromatic amines as well as carboxylic acids. Moreover, especially the *alanine* derived phases **p1** and *ent*-**p1** strongly differentiate the enantiomers of chiral alcohols. Albeit to a lesser, but still significant extend, the same is true for ketones. The smallest effect is seen with the amines. The comparison of the alignment tensors derived from the same analyte enantiomer in both phases (homochiral comparison) suggests a higher contribution of the molecular shape to the orienting mechanism in the **p2**-phase as compared to the **p1**-phase. In most cases these orientational differences are very pronounced but, interestingly, cannot be traced back to the inverted helical sense in these polymers. Further studies to learn more about the complex, multidimensional orienting mechanisms are ongoing.

Experimental Section

Experimental Details for the monomer, polymer and phase preparations as well as sample compositions and tensor comparisons can be found in the Supporting Information.

Acknowledgements

Support from the DFG (Re 1007/8-1 and 1007/9-1), CAPES (418729698) as well as from the Sino-German Center for Research Promotion (GZ1289) is gratefully acknowledged. Open Access funding enabled and organized by Projekt DEAL.

Conflict of Interest

The authors declare no conflict of interest.

Data Availability Statement

The data that support the findings of this study are available from the corresponding author upon reasonable request.

Keywords: anisotropic phases · helical chirality · lyotropic liquid crystals · NMR · polymers

[1] a) M. Köck, M. Reggelin, S. Immel, *Mar. Drugs* **2021**, *19*, 283; b) M. Köck, M. Reggelin, S. Immel, *Mar. Drugs* **2020**, *18*, 330; c) N. Nath, J. C. Fuentes-Monteverde, D. Pech-Puch, J. Rodriguez, C. Jimenez, M. Noll, A. Kreiter, M. Reggelin, A. Navarro-Vazquez, C. Griesinger, *Nat. Commun.* **2020**, *11*, 4372, 9; d) X. L. Li, L. P. Chi, A. Navarro-Vazquez, S. Hwang, P. Schmieder, X. M. Li, X. Li, S. Q. Yang, X. X. Lei, B. G. Wang, H. Sun, *J. Am. Chem. Soc.* **2020**, *142*, 2301–2309; e) Y. Z. Liu, A. Navarro-Vázquez, R. R. Gil, C. Griesinger, G. E. Martin, R. T. Williamson, *Nat. Protoc.* **2019**, *14*, 217–247; f) A. Navarro-Vázquez, R. R. Gil, K. Blinov, *J. Nat. Prod.* **2018**, *81*, 203–210; g) N. Marcó, R. R. Gil, T. Parella, *Magn. Reson. Chem.* **2017**, *55*, 540–545; h) Y. Liu, J. Saurí, E. Mevers, M. W. Peczuh, H. Hiemstra, J. Clardy, G. E. Martin, R. T. Williamson, *Science* **2017**, *356*, 43–50; i) L. Castañar, M. Garcia, E. Hellemann, P. Nolis, R. R. Gil, T. Parella, *J. Org. Chem.* **2016**, *81*, 11126–11131; j) R. R. Gil, C. Griesinger, A. Navarro-Vázquez, H. Sun, in *Structure Elucidation in Organic Chemistry* **2015**, 279–324; k) B. Böttcher, C. M. Thiele, in *eMagRes*, John Wiley & Sons, Ltd, **2012**, pp. 169–180; l) P. Trigo-Mouriño, A. Navarro-Vázquez, J. F. Ying, R. R. Gil, A. Bax, *Angew. Chem. Int. Ed.* **2011**, *50*, 7576–7580; m) G. Kummerlöwe, B. Crone, M. Kretschmer, S. F. Kirsch, B. Luy, *Angew. Chem. Int. Ed.* **2011**, *50*, 2643–2645; n) B. Luy, *J. Indian Inst. Sci.* **2010**, *90*, 119–132; o) C. Gayathri, M. C. de la Fuente, B. Luy, R. R. Gil, A. Navarro-Vázquez, *Chem. Commun.* **2010**, *46*, 5879–5881; p) G. Kummerlöwe, B. Luy, in *Annu. Rep. NMR Spectrosc., Vol. 68* (Ed.: G. A. Webb), **2009**, pp. 193–230; q) G. Kummerlöwe, B. Luy, *TrAC Trends Anal. Chem.* **2009**, *28*, 483–493; r) M. E. García, S. Pagola, A. Navarro-Vázquez, D. D. Phillips, C. Gayathri, H. Krakauer, P. W. Stephens, V. E. Nicotra, R. R. Gil, *Angew. Chem. Int. Ed.* **2009**, *48*, 5670–5674; s) C. M. Thiele, *Eur. J. Org. Chem.* **2008**, 5673–5685; t) J. W. Emsley, J. C. Lindon, *NMR Spectroscopy Using Liquid Crystal Solvents*, Pergamon Press, Oxford, **1975**.

[2] a) G. W. Li, H. Liu, F. Qiu, X. J. Wang, X. X. Lei, *Nat. Prod. Bioprospect.* **2018**, *8*, 279–295; b) G. Cornilescu, R. F. R. Alvarenga, T. P. Wyche, T. S. Bugni, R. R. Gil, C. C. Cornilescu, W. M. Westler, J. L. Markley, C. D. Schwieters, *ACS Chem. Biol.* **2017**, *12*, 2157–2163; c) E. Troche-Pesqueira, C. Anklin, R. R. Gil, A. Navarro-Vázquez, *Angew. Chem. Int. Ed.* **2017**, *56*, 3660–3664; d) P. Tzvetkova, B. Luy, S. Simova, *Magn. Reson. Chem.* **2012**, *50 Suppl 1*, S92–101; e) R. R. Gil, *Angew. Chem. Int. Ed.* **2011**, *50*, 7222–7224; f) C. M. Thiele, *J. Org. Chem.* **2004**, *69*, 7403–7413; g) L. Verdier, P. Sakhaii, M. Zweckstetter, C. Griesinger, *J. Magn. Reson.* **2003**, *163*, 353–359; h) R. R. Gil, *Residual Dipolar Couplings in Small-Molecule NMR*, Academic Press Ltd-Elsevier Science Ltd, London, **2017**.

[3] A. Schütz, J. Junker, A. Leonov, O. F. Lange, T. F. Molinski, C. Griesinger, *J. Am. Chem. Soc.* **2007**, *129*, 15114–15115.

[4] a) G. Bifulco, R. Riccio, G. E. Martin, A. V. Buevich, R. T. Williamson, *Org. Lett.* **2013**, *15*, 654–657; b) C. A. G. Haasnoot, F. Deleeuw, C. Altona, *Tetrahedron* **1980**, *36*, 2783–2792; c) M. Karplus, *J. Chem. Phys.* **1959**, *30*, 11–15.

[5] a) D. Neuhaus, M. P. Williamson, *The Nuclear Overhauser Effect in Structural and Conformational Analysis*, Wiley-VCH, Weinheim, **2000**; b) B. Vögeli, *Prog. Nucl. Magn. Reson. Spectrosc.* **2014**, *78*, 1–46.

[6] a) B. Reif, M. Hennig, C. Griesinger, *Science* **1997**, *276*, 1230–1233; b) B. Reif, H. Steinhagen, B. Junker, M. Reggelin, C. Griesinger, *Angew. Chem. Int. Ed.* **1998**, *37*, 1903–1906; c) C. Griesinger, J. Junker, B. Reif, H. Steinhagen, B. Junker, I. C. Felli, M. Reggelin, *Chem. Eur. J.* **2000**, *6*, 3281–3286.

[7] F. Kramer, M. V. Deshmukh, H. Kessler, S. J. Glaser, *Concepts Magn. Reson. Part A* **2004**, *21 A*, 10–21.

[8] S. Immel, M. Köck, M. Reggelin, *Chem. Eur. J.* **2018**, *24*, 13918–13930.

[9] a) S. Immel, M. Köck, M. Reggelin, *Chirality* **2019**, *31*, 384–400; b) M. Reggelin, S. Immel, *Angew. Chem. Int. Ed.* **2021**, *60*, 3412–3416.

[10] a) D. S. Carvalho, D. G. B. da Silva, F. Hallwass, A. Navarro-Vázquez, *J. Magn. Reson.* **2019**, *302*, 21–27; b) R. R. Gil, C. Gayathri, N. V. Tsarevsky, K. Matyjaszewski, *J. Org. Chem.* **2008**, *73*, 840–848; c) J. Auernheimer, A. Lendlein, B. Luy, *J. Am. Chem. Soc.* **2007**, *129*, 6080–6081; d) J. C. Freudenberger, P. Spiteller, R. Bauer, H. Kessler, B. Luy, *J. Am. Chem. Soc.* **2004**, *126*, 14690–14691; e) T. Montag, C. Thiele, *Chem. Eur. J.* **2013**, *19*, 2271–2274; f) M. Schmidt, H. Sun, A. Leonov, C. Griesinger, U. M. Reinscheid, *Magn. Reson. Chem.* **2012**, *50 Suppl 1*, S38–44; g) G. Kummerlöwe, M. U. Kiran, B. Luy, *Chem. Eur. J.* **2009**, *15*, 12192–12195.

[11] a) I. E. Ndukwe, X. Wang, I. Pelczer, M. Reibarkh, R. T. Williamson, Y. Liu, G. E. Martin, *Chem. Commun.* **2019**, *55*, 4327–4330; b) P. Lesot, P. Berdagué, A. Meddour, A. Kreiter, M. Noll, M. Reggelin, *ChemPlusChem* **2019**, *84*, 144–153; c) S. Jeziorowski, C. M. Thiele, *Chem. Eur. J.* **2018**, *24*, 15631–15637; d) M. Schwab, V. Schmidts, C. M. Thiele, *Chem. Eur. J.* **2018**, *24*, 14373–14377; e) M. Reller, S. Wesp, M. R. M. Koos, M. Reggelin, B. Luy, *Chem. Eur. J.* **2017**, *23*, 13351–13359; f) X. X. Lei, Z. Xu, H. Sun, S. Wang, C. Griesinger, L. Peng, C. Gao, R. X. Tan, *J. Am. Chem. Soc.* **2014**, *136*, 11280–11283; g) N.-C. Meyer, A. Krupp, V. Schmidts, C. M. Thiele, M. Reggelin, *Angew. Chem.* **2012**, *124*, 8459–8463; h) A. Krupp, M. Reggelin, *Magn. Reson. Chem.* **2012**, *50*, S45-S52; i) P. Lesot, J. Courtieu, *Prog. Nucl. Magn. Reson. Spectrosc.* **2009**, *55*, 128–159; j) C. M. Thiele, *Concepts Magn. Reson. Part A* **2007**, *30 A*, 65–80; k) P. Lesot, M. Sarfati, J. Courtieu, *Chem. Eur. J.* **2003**, *9*, 1724–1745; l) C. Aroulanda, V. Boucard, F. Guibe, J. Courtieu, D. Merlet, *Chem. Eur. J.* **2003**, *9*, 4536–4539; m) D. Merlet, B. Ancian, J. Courtieu, P. Lesot, *J. Am. Chem. Soc.* **1999**, *121*, 5249–5258; n) I. Canet, J. Courtieu, A. Loewenstein, A. Meddour, J. M. Pechine, *J. Am. Chem. Soc.* **1995**, *117*, 6520–6526; o) A. Meddour, I. Canet, A. Loewenstein, J. M. Pechine, J. Courtieu, *J. Am. Chem. Soc.* **1994**, *116*, 9652–9656; p) J. P. Bayle, J. Courtieu, E. Gabetty, A. Loewenstein, J. M. Pechine, *New J. Chem.* **1992**, *16*, 837–838.

[12] A. Meddour, P. Berdague, A. Hedli, J. Courtieu, P. Lesot, *J. Am. Chem. Soc.* **1997**, *119*, 4502–4508.

[13] a) K. Czarniecka, E. T. Samulski, *Mol. Cryst. Liq. Cryst.* **1981**, *63*, 205–214; b) M. D. Poliks, Y. W. Park, E. T. Samulski, *Mol. Cryst. Liq. Cryst.* **1987**, *153*, 321–345; c) C. Aroulanda, M. Sarfati, J. Courtieu, P. Lesot, *Enantiomer* **2001**, *6*, 281–287; d) A. Marx, V. Schmidts, C. Thiele, *Magn. Reson. Chem.* **2009**, *47*, 734–740; e) V. Madiot, P. Lesot, D. Gree, J. Courtieu, R. Gree, *Chem. Commun.* **2000**, 169–170; f) S. Hansmann, T. Larem, C. M. Thiele, *Eur. J. Org. Chem.* **2016**, 1324–1329.

[14] L. Arnold, A. Marx, C. Thiele, M. Reggelin, *Chem. Eur. J.* **2010**, *16*, 10342–10346.

[15] a) N.-C. Meyer, A. Krupp, V. Schmidts, C. M. Thiele, M. Reggelin, *Angew. Chem. Int. Ed.* **2012**, *51*, 8334–8338; b) A. Krupp, M. Noll, M. Reggelin, *Magn. Reson. Chem.* **2021**, *59*, 577–586.

[16] K. Kobzar, H. Kessler, B. Luy, *Angew. Chem. Int. Ed.* **2005**, *44*, 3145–3147.

[17] K. Okoshi, K. Sakajiri, J. Kumaki, E. Yashima, *Macromolecules* **2005**, *38*, 4061–4064.

[18] M. Dama, S. Berger, *Org. Lett.* **2012**, *14*, 241–243.

[19] a) J. J. L. M. Cornelissen, J. J. J. M. Donners, R. de Gelder, W. S. Graswinckel, G. A. Metselaar, A. E. Rowan, N. A. J. M. Sommerdijk, R. J. M. Nolte, *Science* **2001**, *293*, 676–680; b) P. H. J. Kouwer, M. Koepf, V. A. A. Le Sage, M. Jaspers, A. M. van Buul, Z. H. Eksteen-Akeroyd, T. Woltinge, E. Schwartz, H. J. Kitto, R. Hoogenboom, S. J. Picken, R. J. M. Nolte, E. Mendes, A. E. Rowan, *Nature* **2013**, *493*, 651–655.

[20] G. W. Li, J. M. Cao, W. Zong, L. Hu, M. L. Hu, X. X. Lei, H. Sun, R. X. Tan, *Chem. Eur. J.* **2017**, *23*, 7653–7656.

[21] a) E. Yashima, K. Maeda, H. Iida, Y. Furusho, K. Nagai, *Chem. Rev.* **2009**, *109*, 6102–6211; b) H. Onouchi, K. Okoshi, T. Kajitani, S. I. Sakurai, K. Nagai, J. Kumaki, K. Onitsuka, E. Yashima, *J. Am. Chem. Soc.* **2008**, *130*, 229–236; c) T. Kajitani, K. Okoshi, S. I. Sakurai, J. Kumaki, E. Yashima, *J. Am. Chem. Soc.* **2006**, *128*, 708–709; d) K. Okoshi, K. Nagai, T. Kajitani, S. I. Sakurai, E. Yashima, *Macromolecules* **2008**, *41*, 7752–7754.

[22] a) K. P. Dhake, P. J. Tambade, R. S. Singhal, B. M. Bhanage, *Green Chem. Lett. Rev.* **2011**, *4*, 151–157; b) I. Ugi, R. Meyr, *Angew. Chem. Int. Ed.* **1958**, *70*, 702–703.
[23] W. Drenth, R. J. M. Nolte, *Acc. Chem. Res.* **1979**, *12*, 30–35.
[24] J. G. Kennemur, B. M. Novak, *Polymer* **2011**, *52*, 1693–1710.
[25] A. Enthart, J. C. Freudenberger, J. Furrer, H. Kessler, B. Luy, *J. Magn. Reson.* **2008**, *192*, 314–322.
[26] G. H. Golub, C. Reinsch, *Numer. Math.* **1970**, *14*, 403–420.
[27] G. Cornilescu, J. L. Marquardt, M. Ottiger, A. Bax, *J. Am. Chem. Soc.* **1998**, *120*, 6836–6837.
[28] E.-J. Wagenmakers, S. Farrell, *Psychon. Bull. Rev.* **2004**, *11*, 192–196.
[29] The GCB for IPC in PBLG and PELG was found to be 0.99 and 0.87, respectively. [S. Hansmann, T. Larem, C. M. Thiele, *Eur. J. Org. Chem.* **2016**, 1324–1329.].

Manuscript received: November 17, 2021
Revised manuscript received: January 2, 2022
Accepted manuscript online: January 5, 2022